Pliocene to Pleistocene vertical movements in the forearc of the Lesser Antilles subduction: insights from chronostratigraphy of shallow-water carbonate platforms (Guadeloupe archipelago)

Philippe Munch, Jean-Jacques Cornee, Jean-Frederic Lebrun, F. Quillevere, C. Verati, M. Melinte-Dobrinescu, F. Demory, Brigitte Smith, F. Jourdan, J. -M. Lardeaux, et al.

Pliocene to Pleistocene vertical movements in the forearc of the Lesser Antilles subduction: insights from chronostratigraphy of shallow-water carbonate platforms (Guadeloupe archipelago)

PH. MÜNCH[1], J.-J. CORNEE[1], J.-F. LEBRUN[2], F. QUILLEVERE[3], C. VERATI[4], M. MELINTE-DOBRINESCU[5], F. DEMORY[6], B. SMITH[1], F. JOURDAN[7], J.-M. LARDEAUX[4], L. DE MIN[2], J.-L. LETICEE[2] & A. RANDRIANASOLO[2]

1Géosciences Montpellier, UMR 5243, Université Montpellier 2, CC 060, place Eugène Bataillon, 34095 Montpellier cedex 5, France
2Equipe LaRGE, Université des Antilles et de la Guyane, BP 592, 97157 Pointe à Pitre Cedex, Guadeloupe, France
3UMR CNRS 5125, 'PaléoEnvironnements & PaléobioSphère', Université Claude Bernard Lyon 1, Campus de la Doua, Bâtiment 'GEODE', 2 rue Raphaël Dubois, 69622 Villeurbanne, France
4Géoazur, Bâtiment 1, 250 rue Albert Einstein, Les Lucioles 1, Sophia-Antipolis, 06560 Valbonne, France
5GeoEcoMar, Str. Dimitri Onciul, nr 23–25, RO-024053, Bucarest, Romania
6CEREGE, UMR 7330, Europôle Méditerranéen de l'Arbois, av. L. Philibert—BP 80, 13545 Aix-en-Provence cedex 04, France
7Western Australian Argon Isotope Facility, Department of Applied Geology & JdL Centre, Curtin University of Technology, GPO Box U1987, Perth, WA 6845, Australia

Abstract: An integrated stratigraphic study was conducted on the shallow water carbonate platforms of the Guadeloupe archipelago to refine the tectonic evolution of the Lesser Antilles forearc. The carbonate platforms are now dated to the Zanclean–Calabrian interval, and their demise occurred between 1.5 and 1.07 Ma. The precise chronostratigraphy allows dating of the main extensional tectonic events since the late Miocene. An initial episode occurred during the late Miocene, related to the reactivation of inherited N130°E-trending shear zones, and led to the emergence of most parts of the forearc. Subsequently, Zanclean to early Piacenzian carbonate platforms developed in association with a general subsidence of the forearc. During the late Piacenzan, a second extensional episode occurred. At this time La Désirade underwent major uplift and emergence whereas most of the forearc remained submerged. Prior to 1.07 Ma, a third north–south extensional episode occurred and led to the final demise of the carbonate platforms. Thus the forearc was characterized by general subsidence since the early Pliocene interrupted by three main extensional episodes and related differential uplifts. This suggests that the Lesser Antilles subduction is probably erosive north of latitude 15°N since *c.* 5 Ma, related to aseismic ridge subduction.

The precise dating of shallow-water carbonate deposits in volcanic arcs developed in plate convergent settings is a major objective for determining the timing of deformation in fore-, intra- and back-arcs, as carbonate platforms record sea-level changes, palaeoclimate and palaeoenvironmental changes, as well as differential tectonic subsidence or uplift. The dating of tectonic changes is often difficult mainly because of a scarcity of reliable biostratigraphic markers in the shallow-water deposits. However, it can be achieved through a multi-disciplinary approach combining biostratigraphy, $^{40}Ar/^{39}Ar$ dating of volcanic layers and magnetostratigraphy (e.g. Cunningham *et al.* 1994; Cornée *et al.* 2006; Oudet *et al.* 2010). In this paper, we present new investigations that demonstrate the reliability of this integrated approach in a case study of the Guadeloupe archipelago that allows us to propose a new tectonostratigraphic model for this part of the Lesser Antilles forearc.

The Guadeloupe archipelago is located in the northern part of the Lesser Antilles forearc (Fig. 1) and formed as the result of the westward subduction of Atlantic oceanic lithosphere beneath the Caribbean Plate (Bouysse *et al.* 1993; Mann *et al.* 1995; De Mets *et al.* 2000; Pindell & Kennan 2009). The archipelago comprises, to the east, four islands topped by Pliocene to Holocene carbonate platforms situated in a forearc setting ('Limestone Carribees': Grande-Terre, La Désirade, Petite-Terre, Marie-Galante) and, to the west, volcanic islands ('Volcanic Carribees': Basse-Terre and Les Saintes) corresponding to the active volcanic arc (Fig. 1) (Andreieff *et al.* 1989; Bouysse *et al.* 1990). The carbonate platforms were deposited upon an Eocene to late Oligocene volcanic arc overlying Mesozoic basement (Bouysse *et al.* 1983, 1990; Bouysse & Westercamp 1990). According to Feuillet *et al.* (2002, 2004), the archipelago underwent both arc-parallel extension and a general 0.35° westward tilting since the late Pleistocene. Arc-parallel

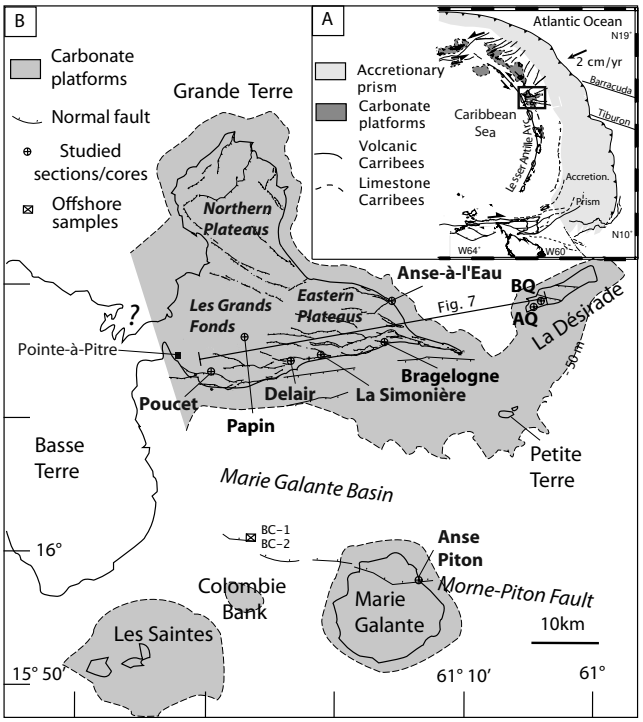

Fig. 1. (**a**) Location of the Guadeloupe archipelago in the Lesser Antilles arc; (**b**) location of the studied sections and dated samples; grey area indicates Pliocene to Recent carbonate platforms. AQ, Airport quarry section; BQ, Beauséjour quarry section.

Fig. 2. Simplified stratigraphic column and sequence stratigraphy of the shallow-water carbonate platforms of Grande-Terre after Andreieff *et al.* (1989), Léticée *et al.* (2005) and Cornée *et al.* (2012).

extension could have resulted from slip partitioning and could have been the cause of the formation of two main grabens, the 2 Ma 'La Désirade trough' and the *c*. 0.5 Ma Marie-Galante graben, which is still active (Feuillet *et al.* 2002). The youngest reefal platforms (present-day 'upper plateaux') may have developed during the *c*. 330 ka highstand over the whole archipelago and an almost synchronous uplift led to their emergence during Marine Isotopic Stage (MIS) 9.3 (Feuillet *et al.* 2004). Subsequently, the whole forearc was uniformly tilted westward by processes unrelated to arc-parallel extension but linked to a transient deformation episode at the subduction interface (Feuillet *et al.* 2004). However, previous studies have suggested that the youngest reefal platforms were much older than 330 ka: late early Pliocene in La Désirade and early Pleistocene in Marie-Galante and in Grande-Terre (Bouysse & Garrabé 1984; Garrabé & Andreieff 1985; Andreieff *et al.* 1989). Moreover, Bouysse & Westercamp (1990) linked the deformation of forearc (north of 15°N) to the subduction of aseismic oceanic ridges, two of which occur in this part of the arc. The Tiburon ridge is located in the south and the Barracuda ridges in the north (Fig. 1). Ridge subduction may have started during the late Oligocene and is likely to have caused a temporary cessation of subduction as well as relocating volcanic activity from an older arc corresponding to the Limestone Carribees to its present-day position (Fig. 1a; Bouysse & Westercamp 1990). Moreover, those researchers proposed that (1) emergence of islands in the Guadeloupe archipelago occurred diachronously, first in La Désirade during the late Pliocene, then in Marie-Galante during the Pleistocene and lastly in Grande-Terre also during the Pleistocene, and (2) La Désirade was tilted northeastward whereas the other forearc islands were tilted westward. Indeed, subduction of aseismic ridges is known to be associated with erosion of the base of the overriding plate and to trigger extensional deformation and subsidence of the forearc (e.g. Clift & Vannucchi 2004, and references therein). Subsidence of a forearc may be 'the best proxy' of subduction erosion (Vannucchi *et al.* 2013).

There are two key aims of this work. The first is to establish for the first time a precise dating for the growth and demise of the Pliocene–Pleistocene shallow-water carbonate platforms of the Lesser Antilles forearc by means of integrated stratigraphy (planktonic foraminifer and calcareous nannoplankton biostratigraphy, $^{40}Ar/^{39}Ar$ dating of volcaniclastic layers and magnetostratigraphy). The second is to establish a refined timing of subsidence and uplift events of the Lesser Antilles forearc in the Guadeloupe region. These allow us to discuss whether Pliocene–Pleistocene extensional deformation of the forearc is related to slip partitioning or to subduction erosion. The timing and the duration of vertical motions that affected the carbonate platforms are also an important matter of debate to constrain slip rates of Quaternary deformations and seismic hazards in the Guadeloupe archipelago.

Stratigraphy of carbonate platforms

The litho- and biostratigraphy of the carbonate platforms have been mainly investigated in Grande-Terre. Following the investigations of Andreïeff *et al.* (1983, 1989), Garrabé & Andreieff (1985), Garrabé & Andreieff (1988) and Léticée *et al.* (2005) the carbonate platforms can be divided into five sedimentary units (Fig. 2). Unit 1, up to 75 m thick, corresponds to red algal shallow-water rudstone to boundstone (Calcaires inférieurs à rhodolites Formation) changing eastward into planktonic foraminifer-rich wackestone to packstone dated to Zones PL2–PL5 of Berggren *et al.* (1995) (early Pliocene–early Pleistocene interval). Unit 2 is a volcaniclastic unit (Formation Volcano-sédimentaire) enriched in rhodoliths and dates from Zone PL5 (early Pleistocene). It crops out over the whole Grande-Terre Island and it is considered as a stratigraphic index bed. Unit 3 is composed of red algal shallow-water rudstone to boundstone (Calcaires supérieurs à rhodolites Formation) and is dated to Zones PL6–Pt1a (late early–middle Pleistocene interval). Unit 4 corresponds to a prograding reefal platform up to 30 m thick

that yielded a coral assemblage dominated by *Agaricia* sp. (Calcaires à Agaricia Formation). Unit 5, only recently described (Léticée *et al.* 2005), is composed first by a retrograding coarse-grained member (Unit 5a) and then by a 15 m thick reefal platform dominated by *Acropora palmata* (Unit 5b; Calcaires à Acropora Formation). This unit corresponds to the 'upper plateaux' of Grande-Terre and Marie-Galante as defined by Feuillet *et al.* (2002, 2004) and it also crops out on Petite-Terre. The age of Units 4 and 5 remains poorly constrained. It may correspond to Zone Pt1a (middle Pleistocene; i.e. between 1.81 and 0.78 Ma) according to the study of the La Simonière core by Andreieff *et al.* (1989), whereas Unit 5 may be dated at *c*. 330 ka (late Pleistocene) according to Feuillet *et al.* (2002, 2004).

Recently, Cornée *et al.* (2012) and Lardeaux *et al.* (2013) showed that the carbonate platforms of Grande-Terre and La Désirade comprise four sedimentary sequences separated by erosional unconformities (Fig. 2). Sequences S1 and S2 correlate with Unit 1 and are topped by the sequence boundaries SB0 and SB1, respectively. Both sequences are incomplete and display only aggrading pattern, suggesting that erosional SB0 and SB1 were generated by local tectonic uplifts. Biostratigraphic data of Cornée *et al.* (2012) for the top of sequence S2 and the base of sequence S3 in the Anse à l'Eau section (Fig. 2) are in accordance with those of Andreieff *et al.* (1989). Sequence S3 encompasses Units 2–4 and it is topped by a major erosional surface (SB2). Sequence S4 correlates with Unit 5 and its top corresponds to the present-day topography (SB3). The youngest two sequences exhibit a complete transgressive–regressive sedimentary pattern suggesting a response to sea-level changes. Thus, according to Cornée *et al.* (2012), the first two sequences may be related to tectonic events whereas the last two may have a eustatic origin related to the onset of glaciations within the Northern Hemisphere. They suggested that S3 could be correlated with the Ge2 eustatic cycle and S4 with the Cala1 or Cala2 eustatic cycles (Haq *et al.* 1988).

In this work, to perform an integrated stratigraphy of forearc carbonate platforms, we mainly studied five sections arranged along a profile perpendicular to the arc (Fig. 1). We applied magnetostratigraphy in three of them (Poucet, Papin and Delair sections) and new biostratigraphic determinations in three (Poucet, Bragelogne and Airport quarry sections). We also performed $^{40}Ar/^{39}Ar$ dating of five volcaniclastic tuffs: two in Grande-Terre (Bragelogne and Anse à l'Eau sections), one in Marie-Galante (Anse Piton) and two in the offshore domain near the Colombie Bank (Fig. 1). The Bragelogne section in Grande-Terre and the Airport quarry section in La Désirade were not investigated in previous studies. The Bragelogne section is the only one in Grande-Terre where sequence S2 is missing beneath the SB1 unconformity. The volcaniclastic deposits of sequence S3 (Unit 3) directly onlap onto sandy marlstones of sequence S1 (Unit 1), related to the erosion of the footwall high of a N130°E-striking normal fault (Fig. 1). The activity of the normal fault appears to slightly predate the deposition of sequence S3. The Airport quarry section allows a refinement of the biostratigraphy for sequence S2 in La Désirade (location in Fig. 1).

Biostratigraphy

Eighteen samples were collected from two new sections for calcareous nannofossil and planktonic foraminiferal biostratigraphic analyses (Fig. 1). Samples were collected from Grande-Terre within sequences S1–S3 (Bragelogne) and from the western part of La Désirade within sequence S2 (Airport quarry). Because of poor preservation of microfossils in the volcaniclastic sediments, three additional samples were also taken from the base of sequence S3 in the Poucet section (Fig. 1) to confirm previous determinations.

For planktonic foraminiferal stratigraphy, samples were washed through a 65 µm sieve. The residue was dry-sieved and the size fractions coarser than 150 µm were used for further investigations. Specimens were picked under a Wild Heerbrugg binocular microscope and identified following the taxonomic concepts and nomenclature of Kennett & Srinivasan (1983). For calcareous nannofossil analyses, standard smear slides were prepared from the samples. Analyses were performed with a light polarizing Nikon23 microscope at 1600× magnification. The nannofloral taxonomic identification follows Perch-Nielsen (1985) and Young *et al.* (2003). Because of the poor to moderate preservation of the planktonic foraminifers and calcareous nannoplankton (only the seven samples from the Airport quarry section yielded determinable nannoplankton), analyses are based on a complete inventory of species within the samples, to better characterize the occurrence of stratigraphically significant taxa. Biostratigraphic ages are based on Wade *et al.* (2011) for planktonic foraminifers and Raffi *et al.* (2006) for calcareous nannofossils.

In the Bragelogne section (Grande-Terre), samples located below SB1 (Unit 1) yielded planktonic foraminifersl assemblages that indicate Zones PL2–PL3 of Berggren *et al.* (1995). In all these samples, the occurrence of *Dentoglobigerina altispira* (Last Appearance Datum (LAD) = 3.13 Ma) indicates an early Piacenzian (or late Pliocene) age at youngest. In the three lowermost samples, the co-occurrence of *Menardella exilis* (First Appearance Datum (FAD) = 4.45 Ma; LAD = 2.09 Ma) and *D. altispira* (LAD = 3.13 Ma) indicates a late Zanclean–early Piacenzian age at oldest. In the two volcaniclastic samples located above SB1, the occurrence of *Menardella miocenica* (FAD = 3.77 Ma; LAD = 2.39 Ma), together with the absence of *D. altispira* (LAD = 3.13 Ma), points to Zone PL5 in the late Piacenzian to early Gelasian.

In the Poucet section (Grande-Terre), our results are in agreement with those of Cornée *et al.* (2012). The volcaniclastic deposits from the base of sequence S3 (Unit 2), located directly above SB1 at the base of sequence S3, date from the late Piacenzian–early Gelasian (Zone PL5) because of the co-occurrence of *M. miocenica* (LAD = 2.39 Ma) and *Menardella multicamerata* (LAD = 2.99 Ma), and the absence of *D. altispira* (LAD = 3.13 Ma). That is the same age as in the upper part of the Bragelogne section.

In the Airport quarry section (La Désirade), all samples yielded planktonic foraminiferal assemblages that point to Zone PL3. The co-occurrence of *D. altispira* (LAD = 3.13 Ma), *Sphaerodinellopsis semulina* (LAD = 3.16 Ma), *Pulleniatina* sp. (Atlantic disappearance = 3.41 Ma) and *Menardella pertenuis* (FAD = 3.52 Ma) indicates an early Piacenzian age. The same samples also yielded calcareous nannofossils that indicate Zone NN16 (Martini 1971) and Zones CN11b–CN12a (Okada & Bukry 1980). The co-occurrence of *Discoaster tamalis* (Highest Occurrence (HO) = 2.801 Ma) and *Pseudoemiliania lacunosa* (Lowest Occurrence, below the HO of *Reticulofenestra pseudoumbilicus* at 3.81–3.82 Ma) together with the absence of *Sphenolithus* spp. (HO = 3.52–3.56 Ma) indicate a Piacenzian age. That is the same age as in the Beauséjour quarry section in La Désirade (Lardeaux *et al.* 2013) and as the upper part of sequence S1 (Unit 1) in Grande-Terre (Andreieff *et al.* 1989; Cornée *et al.* 2012).

$^{40}Ar/^{39}Ar$ dating

Crystals of plagioclase from five volcaniclastic layers were analysed by $^{40}Ar/^{39}Ar$ step-heating experiments in the Géoazur laboratory (Nice, France), in the Western Australian Argon Isotope Facility (Curtin University, Perth) and in the Géosciences Montpellier laboratory (Montpellier, France). Both furnace and integrated laser procedure were used. After magnetic and standard

Table 1. *Summary of plateau and isochron $^{40}Ar/^{39}Ar$ ages obtained from plagioclase samples by furnace treatment*

Laboratory run	Standard	Sample	Plateau age (Ma)	±	2σ	% ^{39}Ar	MSWD	*P*	Inverse isochron age (Ma)	±	2σ	$^{40}Ar/^{36}Ar$ intercept	±	2σ	MSWD	*P*
A	GA-1550	AP-1	8.57	±	0.43	99.9	1.06	0.39	8.60	±	0.52	297	±	9	1.14	0.32
C	FCS	BRA-9-1B	2.89	±	0.19	100	0.64	0.81	2.82	±	0.22	309	±	16	0.52	0.96
M1869	ACs	ALE-7	1.96	±	0.17	97.7	0.06	1.00	2.04	±	0.29	281	±	55	0.06	1.00
D	GA-1550	BC-1	1.50	±	0.34	96.2	0.84	0.61	1.64	±	0.40	293	±	13	0.99	0.45
E	GA-1550	BC-1	1.20	±	0.30	90.8	0.82	0.61	1.07	±	0.38	304	±	11	0.81	0.60
D + E combined	GA-1550	BC-1	1.33	±	0.23	92.6	0.87	0.65	1.34	±	0.26	299	±	8	0.99	0.47
G	GA-1550	BC-2	1.11	±	0.19	85.6	1.09	0.35	1.02	±	0.2	308	±	10	0.86	0.57
F	GA-1550	BC-2	1.18	±	0.16	100	0.94	0.52	1.12	±	0.18	304	±	9	0.93	0.52
G + F combined	GA-1550	BC-2	1.15	±	0.12	93.2	0.98	0.49	1.08	±	0.14	306	±	7	0.85	0.68

Samples A–G were analysed at Curtin University, and M1869 at Nice Géoazur laboratory. Equipment and experimental techniques used at Géoazur were as described by Cornée *et al.* (2006). Cd-shielded samples were co-irradiated for 1.2 or 2 h in the nuclear reactor at McMaster University (Hamilton, Canada), in position 5c, along with Alder Creek Sanidine (ACs-2), Fish Canyon Sanidine (FCS) or GA1550 biotite neutron fluence monitors for which an age of 1.2061 ± 0.002 Ma, 28.305 ± 0.036 Ma or 99.769 ± 0.110 Ma respectively was adopted (Renne *et al.* 2010). All argon age data were calculated (and corrected) using the new K decay constant of 5.5492×10^{-10} a^{-1} reported by Renne *et al.* (2010). The samples analysed at Curtin University were step-heated in a double-vacuum high-frequency Pond Engineering furnace. The gas was purified in a stainless steel extraction line using a GP50 and two AP10 SAES getters and a liquid nitrogen condensation trap for 10 min. Ar isotopes were measured in static mode using a MAP 215-50 mass spectrometer with a Balzers SEV 217 electron multiplier. Raw data were processed using the ArArCALC-software (Koppers 2002) and the ages were calculated using the decay constants recommended by Renne *et al.* (2010). J-values computed from standard grains: 0.000699 ± 0.29 to 0.000707 ± 0.71% for samples analysed at Curtin University; 0.000276 ± 0.5% for the sample analysed at Géoazur, Nice. Mass discrimination was monitored using an automated air pipette and provided a mean value of 1.00646 ± 0.00238 per dalton (Curtin University, Perth) and 1.00564 ± 2% at 1σ (Géoazur, Nice). The correction factors for interfering isotopes were $(^{39}Ar/^{37}Ar)_{Ca} = 7.30 \times 10^{-4}$ (±11%), $(^{36}Ar/^{37}Ar)_{Ca} = 2.82 \times 10^{-4}$ (±1%), $(^{40}Ar/^{39}Ar)_{K} = 6.76 \times 10^{-4}$ (±10%; Curtin University, Perth) and $(^{40}Ar/^{39}Ar)_{K} = 10^{-3}$ (±3%; Géoazur, Nice). Our criteria for the determination of a plateau are as follows: the plateau must include at least 70% of ^{39}Ar; the plateau should be distributed over a minimum of three consecutive steps agreeing at 95% confidence level and satisfying a probability of fit (*P*) of at least 0.05.

heavy liquid separations of a 100–200 µm powder, 150–300 mg of transparent plagioclase was handpicked under a binocular microscope. The grains were leached with HNO_3 (1N) for a few minutes and then repeatedly cleaned ultrasonically in distilled water. We sampled 150–250 mg of plagioclase bulk sample for furnace experiments and *c*. 70 grains aliquot for the laser method. Equipment and experimental techniques are described in Table 1. Synthesized results are given in Figure 3 and Table 1. All data reported in the text and in the figures are at the 2σ confidence level.

Sample AP-1 (Anse Piton, Marie-Galante, basement of the carbonate platform; Figs 1 and 3a). The plagioclase bulk sample yielded a well-defined plateau age at 8.57 ± 0.43 Ma corresponding to 99% of ^{39}Ar released. The inverse isochron calculation yielded an identical age at 8.6 ± 0.52 Ma (mean standard weighted deviation (MSWD) = 1.14) with an initial $^{40}Ar/^{36}Ar$ ratio at 297 ± 9 indicating that the trapped $^{40}Ar/^{36}Ar$ is indistinguishable from atmospheric $^{40}Ar/^{36}Ar$. A total fusion (after a pre-degassing step) was also performed on a micro-population and yielded an integrated age of 8.83 ± 0.24 Ma that is concordant with the step-heated age. We consider the plateau age of 8.57 ± 0.43 Ma as the best estimate for these volcaniclastic sediments.

Sample BRA-09-1b (Bragelogne, Grande-Terre, base of the sequence S3/Unit 2; Figs 1 and 3b). The plagioclase bulk sample yielded a well-defined plateau age at 2.89 ± 0.19 Ma corresponding to 100% of ^{39}Ar released. The inverse isochron yielded an identical age at 2.82 ± 0.22 Ma (MSWD = 0.52) with an initial $^{40}Ar/^{36}Ar$ ratio of 309 ± 16 near the atmospheric ratio. We consider the plateau age of 2.89 ± 0.19 Ma as the best estimate of this volcaniclastic layer.

Sample ALE-7 (Anse à l'Eau, Grande-Terre, upper part of the sequence S3/Unit 4; Figs 1 and 3c). The plagioclase bulk sample yielded a well-defined plateau age at 1.96 ± 0.17 Ma (93.4% of ^{39}Ar released). The inverse isochron calculation yielded a less well-constrained but concordant age at 2.02 ± 0.29 Ma (MSWD = 0.06) with an initial $^{40}Ar/^{36}Ar$ ratio of 281 ± 55 concordant with the atmospheric ratio. A duplicate experiment performed with the integrated laser heating system gives a less accurate result (not shown), a plateau age at 1.77 ± 0.40 Ma, although it is concordant with the furnace experiment. This plateau age is not well constrained owing to smaller detected gas fractions (total mineral weight less than 0.8 mg). Below, we consider the plateau age of 1.96 ± 0.17 Ma as the best estimate of the age of this volcaniclastic layer.

Samples BC-1 and BC-2 (Colombie bank, offshore, near the top of sequence S4/Unit 5; Figs 1 and 3d, e). Both samples are foraminiferal wackestones with up to 40% euhedral plagioclase crystals of probable magmatic air-fall origin. They correspond to 'crystal tuffs' as defined by Cas & Wright (1988). Plagioclase bulk samples were analysed in duplicate in both samples. Sample BC-1 yielded two concordant well-defined plateau ages at 1.50 ± 0.34 Ma (BC-1D) and 1.20 ± 0.3 Ma (BC-1E) corresponding to 96.2% and 90.8% of ^{39}Ar released, respectively. The step at 1080 °C for BC-1D, yielding a non-concordant age, is not included in the plateau and inverse isochron age calculation because it would correspond to a decrepitated inclusion. The inverse isochron calculations yielded ages at 1.64 ± 0.40 Ma (MSWD = 0.99; initial $^{40}Ar/^{36}Ar$ ratio at 293 ± 13) and 1.07 ± 0.38 Ma (MSWD = 0.81; initial $^{40}Ar/^{36}Ar$ ratio at 304 ± 11) respectively. The combination of duplicate analyses yielded a plateau age at 1.33 ± 0.23 Ma (92.6% of ^{39}Ar released) and an inverse isochron age of 1.34 ± 0.26 Ma (MSWD = 0.99) with an initial $^{40}Ar/^{36}Ar$ ratio at 299 ± 8 indicating that the trapped $^{40}Ar/^{36}Ar$ is indistinguishable from atmospheric $^{40}Ar/^{36}Ar$. Sample BC-2 yielded also two well-defined concordant plateau ages at 1.11 ± 0.19 Ma (BC-2F) and 1.18 ± 0.16 Ma (BC-2G) corresponding to 85.6% and 100% of ^{39}Ar released, respectively. Inverse isochron calculations yielded ages at 1.02 ± 0.20 Ma (MSWD 0.86; initial $^{40}Ar/^{36}Ar$ ratio at 308 ± 10) and 1.12 ± 0.18 Ma (MSWD 0.93; initial $^{40}Ar/^{36}Ar$ ratio at 304 ± 9). The combination of all steps from the duplicate analyses of BC-2 yielded a plateau age at 1.15 ± 0.12 Ma (93.2% of ^{39}Ar released) and an inverse isochron age at 1.08 ± 0.14 Ma (MSWD 0.85; initial $^{40}Ar/^{36}Ar$ ratio at 306 ± 7). All single ages are concordant at the 2σ level and we retain the combined plateau ages at 1.33 ± 0.23 Ma and 1.15 ± 0.12 Ma for BC-1 and BC-2, respectively.

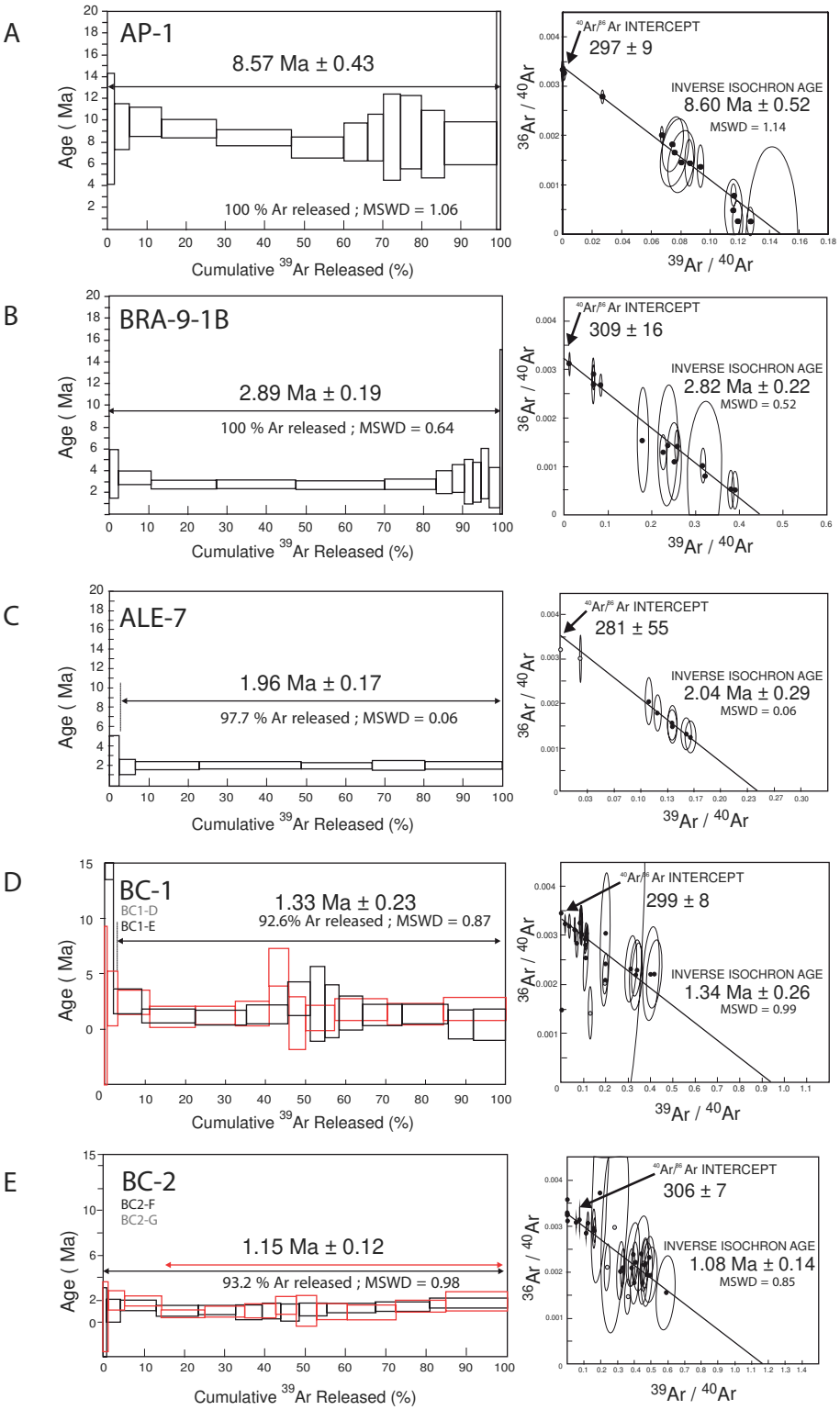

Fig. 3. Degassing spectra for $^{40}Ar/^{39}Ar$ age analysis and related inverse isochron diagrams. $^{40}Ar/^{36}Ar$ intercept values, mean standard weighted deviation and probability of fit (*P*) values are reported. Calculations are determined by using the ArArCALC-software of Koppers (2002).

Magnetostratigraphy of the Grande-Terre carbonate platform

Sampling strategy

To identify Pliocene–Pleistocene geomagnetic polarity reversals in sediments from Grande-Terre, a total of 127 samples was collected from three quarries in Grande-Terre: Papin, Poucet and Delair (Fig. 1). These sections represent a cumulative thickness of 97 m, allowing us to maximize the magnetostratigraphic resolution of the sampling. The sampling was homogeneously distributed along the sections, giving a mean sampling resolution of about 0.7 m, except for the Delair quarry where poor outcrop conditions lead to a 7 m gap in the upper part of the section. For the Poucet

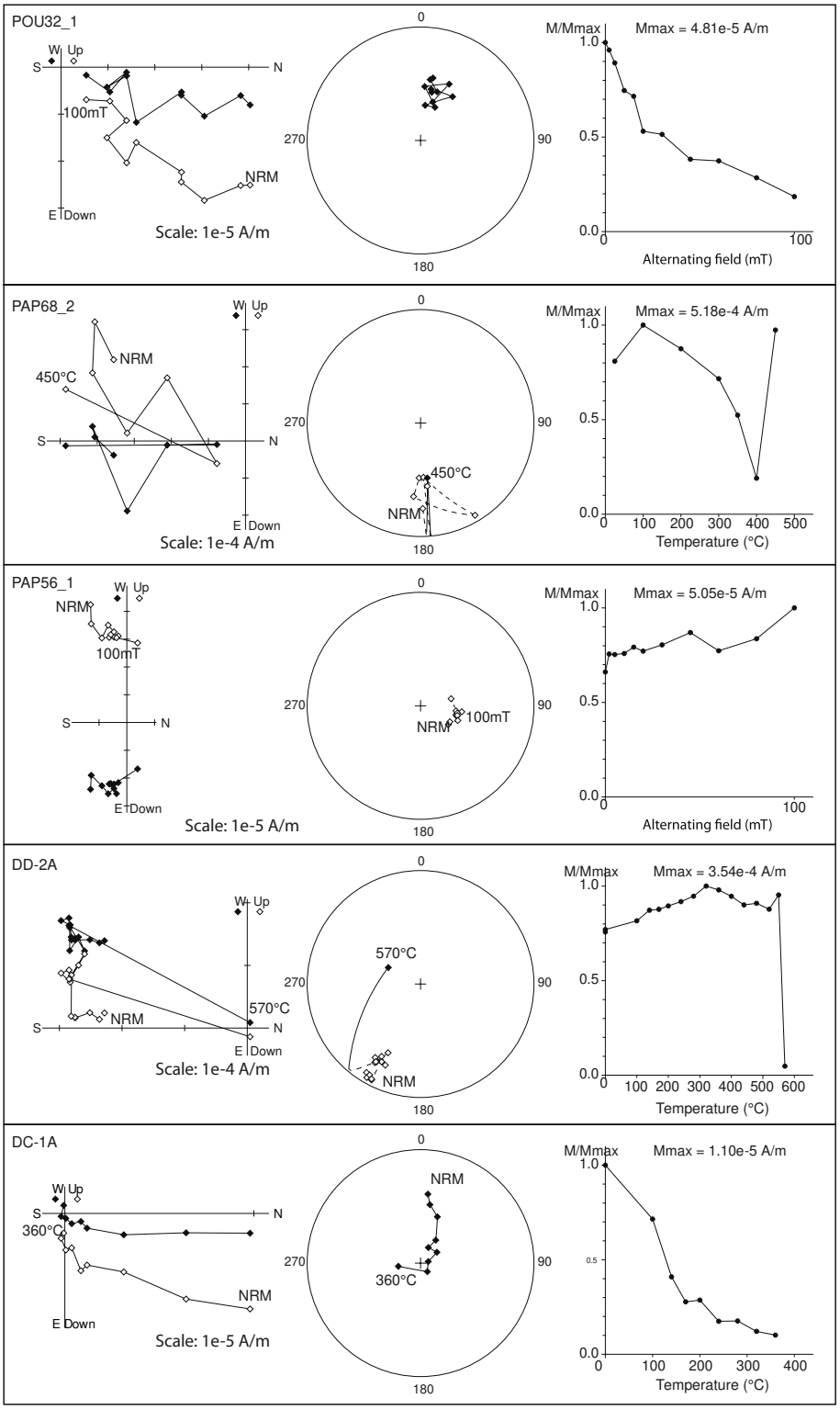

Fig. 4. Demagnetization patterns for selected samples subjected either to thermal demagnetization or to alternating field demagnetization. From left to right: orthogonal projection (Zijderveld 1967), stereographic projection and normalized intensity of the remanent magnetization v. demagnetization treatment.

and Papin sections, samples were collected directly in the field using a Pomeroy Core Drill. The cores are samples of 1 inch (2.54 cm) diameter. They were sliced into 2.2 cm standard length specimens. Fifty-five and 102 specimens were then prepared from the Poucet and the Papin sections, respectively. In the Delair section, eight oriented blocks were collected in the field. Two or three samples were drilled out of each block, and each sample was sliced into two specimens of standard size (2.54/2.2 cm). A total of 36 specimens was thus obtained.

Palaeomagnetic analyses

For the Poucet and Papin sections, samples were measured using the Supraconducting Rock Magnetometer (2G Enterprises, Model

SRM760R) of the CEREGE (Aix-en-Provence, France). The natural remanent magnetization was measured and subject either to stepwise alternating field (AF) demagnetization up to 100 mT, or to stepwise thermal demagnetization up to 450 °C. For the Poucet section, measurements were carried out on 55 specimens: 36 with alternating field demagnetization and 19 with thermal demagnetization. For the Papin section, measurements were performed on 102 specimens: 63 with alternating field demagnetization and 39 with thermal demagnetization. The 36 specimens from the Delair section were measured using the Supraconducting Rock Magnetometer (2G Enterprises) of Montpellier University. Half the specimens were AF demagnetized up to 20 mT using 2 mT steps, then if possible, up to a maximum field of 40 mT every 4 mT. The other half was thermally demagnetized by steps of 100, 140, 170, 200, 240, 280, 320, 360, 400 °C, and for one sample (DD) up to 440, 480, 520 and 570 °C.

For the Poucet and Papin sections, results on 32 and 66 samples could be exploited, respectively. A characteristic remanent magnetization (ChRM) was calculated for each sample using the statistical analysis of Kirschvink (1980) when the demagnetization process was efficient and the direction stable (POU32_1 and PAP68_2 in Fig. 4). We consider that this ChRM reflects a detrital remanent magnetization. Possible lock-in depth of the paleomagnetic record, responsible for a gap of few thousand years as estimated in recent carbonates (Menabreaz *et al.* 2010), is not significant regarding the time scale of the present study. The thermal demagnetization pattern displays artificial remagnetization at step 450 °C owing to mineralogical change during heating (PAP68_2 in Fig. 4). Some samples present a stable component that was hard to demagnetize using alternating field (PAP56_1 in Fig. 4). In such cases, the ChRM was determined using Fisher (1953) statistics. Four types of ChRM were distinguished based on the quality of their directions. Types 1 and 2 are good and medium quality with low and moderate error on ChRM directions respectively (Fig. 5a and b). Only these two types of direction were used to establish the magnetostratigraphic scales in the studied sections. Type 3 directions have highly scattered directions that provide ambiguous polarity determinations. Type 4 directions were not exploitable. Directions were interpreted in terms of geomagnetic polarity only when at least two successive samples presented a similar direction. Polarity scales without gaps and with few uncertainties were built up from the results presented in Figure 5. The Papin section revealed a normal–reverse–normal–reverse polarity sequence with a long reverse magnetozone in the upper part of the section (Fig. 5a). The Poucet section revealed five reversals with a main reverse–normal–reverse–normal polarity pattern (Fig. 5b). However, the lowermost reverse polarity interval was only inferred from the correlation with the Papin section. Also, a short normal polarity interval occurred in the reverse magnetozone from the middle part of the section.

For the Delair section, 32 out of the 36 specimens provided significant results. With the exception of the coarse-grained and unconsolidated sample De3-1a, which was totally remagnetized by a strong VRM (viscous remanent magnetization) as demonstrated by a viscosity test (Prevot 1981), all of the specimens revealed an overall reversed polarity (Fig. 4). However, the great majority of demagnetization paths provided only great circles evolving toward a reverse polarity (DC-1A in Fig. 4). A ChRM (Kirschvink 1980) could be retrieved from only nine specimens, four of which belong to the same block (DB). One sample could reach high temperature without remagnetization (DD-2A in Fig. 4). This sample shows stable reverse polarity up to 550 °C. At this temperature, the remanent signal decreases by more than 90%, but the direction becomes meaningless. It corresponds to the Curie temperature of magnetite, which carries the remanence in this case. This interpretation is supported by the susceptibility changes upon heating, and by the reversibility of the heating and cooling curves. The intersection of the remagnetizing circles, alone or combined with ChRMs, was calculated according to McFadden & Elhinny (1988). At the block level (Fig. 5c), the average direction is poorly defined because the number of reliable specimens is only three or four per block. To obtain a more meaningful statistical value of the average direction, we grouped the blocks on the basis of stratigraphical arguments.

Correlation to the Geomagnetic Polarity Time Scale (GPTS)

Despite major erosional surfaces that may correspond to time gaps, the correlation of the upper part of the composite magnetostratigraphy to the GPTS of Lourens *et al.* (2004) can be proposed, based on the distinctive pattern of polarity reversals and on biochronological constraints from the Poucet section (Fig. 6). Assuming that deposition of the Formation Volcano-sédimentaire (base of the sequence S3/Unit 2) took place in Zone PL5, the normal magnetozone above SB1 can be unambiguously correlated to Subchron C2An.1n (Gauss). Therefore, the two overlying magnetozones correlate with Chrons C2r and C2n, respectively. The short normal polarity interval within Chron C2r can then be correlated with Subchron C2r.1n (Réunion). Despite the unknown hiatus associated with SB2, the inverse magnetozone from the uppermost part of the composite section can be correlated only with Chron C1r. The sampling gap in the upper part of the section did not allow us to determine if the section ended before or after the normal Subchron C1r.1n (Jaramillo). However in all cases, deposition of the uppermost part of the section occurred before Chron C1n (Brunhes); that is, before 780 ka.

Finally, assuming that the lower part of the composite section (Papin section) may date from the late Zanclean–early Piacenzian (Zones PL2–PL3), we propose that the two normal magnetozones recovered in the Papin section correlate with Chrons C2An.2n and C2An.3n, respectively.

Age and duration of the shallow-water carbonate platforms

By combining magnetostratigraphy with biostratigraphic and chronostratigraphic constraints from other studied sections in the whole archipelago, we are able to correlate the composite magnetostratigraphic scale with GPTS (Figs 6 and 7).

Sequences S1 and S2

The age of the base of the carbonate platforms was estimated as earliest Pliocene at Marie-Galante (Zones PL1–PL2 of Andreieff *et al.* 1983). There, the platform rests upon upper Tortonian volcaniclastic marine sediments (Andreieff *et al.* 1983) whereas it rests on a Mesozoic basement at La Désirade (Mattinson *et al.* 1980, 2008; Westercamp 1980; Bouysse *et al.* 1983; Andreieff *et al.* 1989; Cordey & Cornée 2009; Corsini *et al.* 2011; Lardeaux *et al.* 2013). The $^{40}Ar/^{39}Ar$ age of the volcaniclastic marine sediments from the basement in Marie-Galante (8.57 ± 0.43 Ma) indicates that the unconformity between the basement and the overlying carbonates corresponds to a major hiatus of 3.3 myr assuming an age of 5.33 Ma for the base of the carbonate platform. The upper part of sequence S2 (Unit 1) was previously dated as late Piacenzian–early Gelasian in the Anse à l'Eau section (Zone PL5 of Cornée *et al.* 2012) allowing us to propose that the reverse

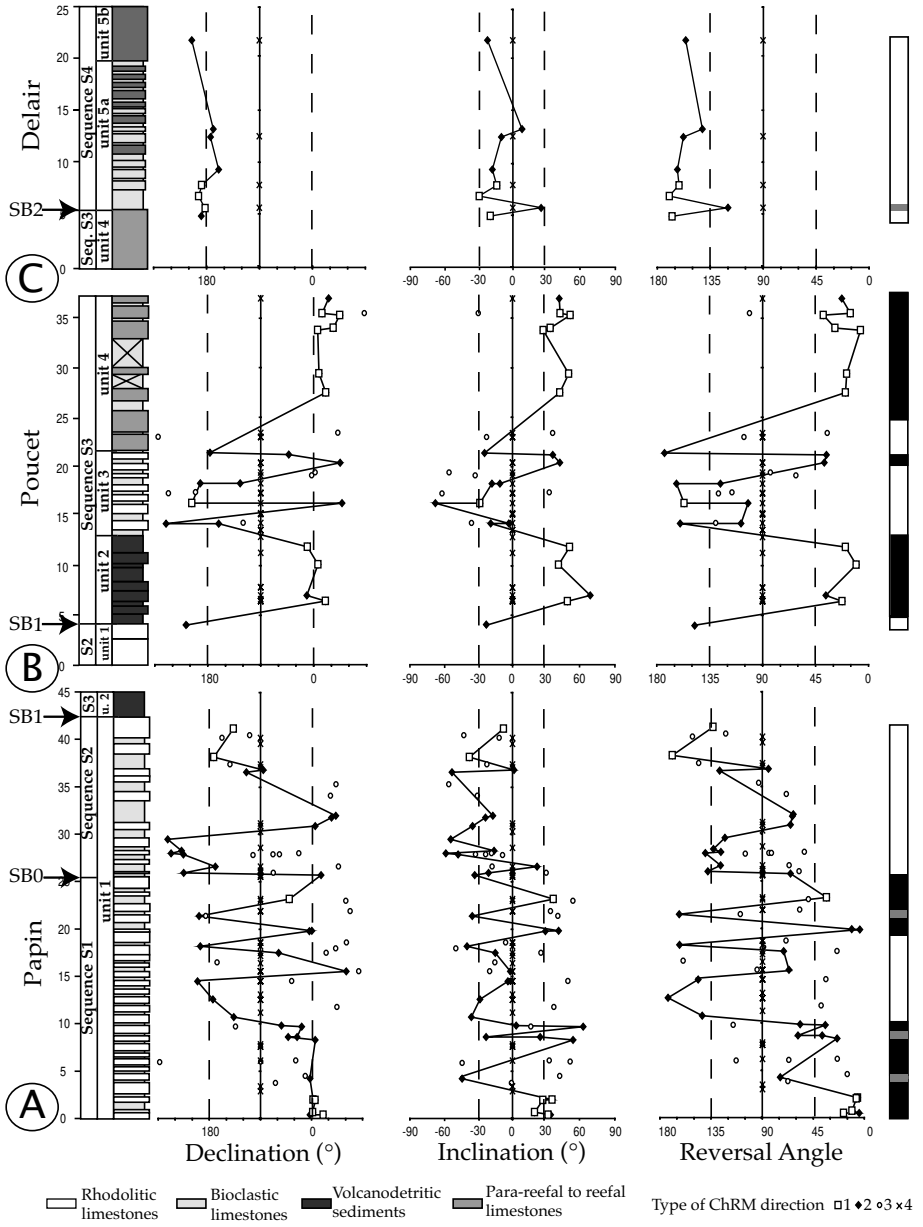

Fig. 5. Stratigraphic columns, magnetostratigraphic results for the studied sections and magnetic polarity sequences. (**a**) Papin section; (**b**) Poucet section; (**c**) Delair section.

magnetozone in the upper part of the Papin section correlates with Chron C2An.1r. Our magnetostratigraphic results help to date the SB0 unconformity as it falls at the base of the reverse magnetozone correlated with Chron C2An.1r. It can then be dated at around 3.1 Ma. As the accumulation rate appears rather constant (*c.* 8 cm ka^{-1}; Fig. 6b) during sequences 1 and 2 (Unit 1), SB0 may correspond to a short-duration hiatus. In Grande-Terre, S2 thus lasted a maximum of 70 kyr (i.e. the duration of Subchron C2An.1r) whereas S1 lasted around 500 kyr (Figs 6 and 7).

Sequence S3

Based on the age of the sample BRA-09-1b (2.89 ± 0.19 Ma) and the absence of *Menardella multicamerata* (LAD = 2.99 Ma in Wade *et al.* 2011), we find that the age of the base of S3 (base of Unit 2) falls between 2.9 and 3 Ma in the Bragelogne section. Thus, the unconformity SB1 corresponds to a hiatus of at most 140 kyr (Fig. 6b). Following the correlation of magnetozones with the GPTS (Fig. 6), we can precisely determine the the duration of the units of sequence S3, as follows.

Unit 2 (volcaniclastic deposits) entirely falls within Subchron C2An.1n and consequently lasted a maximum of 400 kyr between 3 and 2.6 Ma (late Piacenzian).

The top of the Unit 3 falls at the base of Subchron C2r.1r. Unit 3 lasted a maximum of 450 kyr between 2.6 and 2.15 Ma (Gelasian).

The top of Unit 4 (prograding reefs unit) falls near the top of Chron C2n. Thus, Unit 4 lasted a maximum of 370 kyr between 2.15 and 1.77 Ma (latest Gelasian–earliest Calabrian). Consequently, the whole of sequence S3 ended at 1.77 Ma at youngest and lasted a maximum of 1.23 Ma.

In the Anse à l'Eau section, Unit 3 is separated from Unit 2 by a hardground that may correspond to a depositional hiatus of 400–800 kyr according to Cornée *et al.* (2012). The ^{40}Ar/^{39}Ar age at 1.96 ± 0.17 Ma for the crystal tuff ALE-7, corresponding to the first deposits over the hardground, indicates that the whole of Unit 3 and the base of Unit 4 are absent in this section and that the duration of

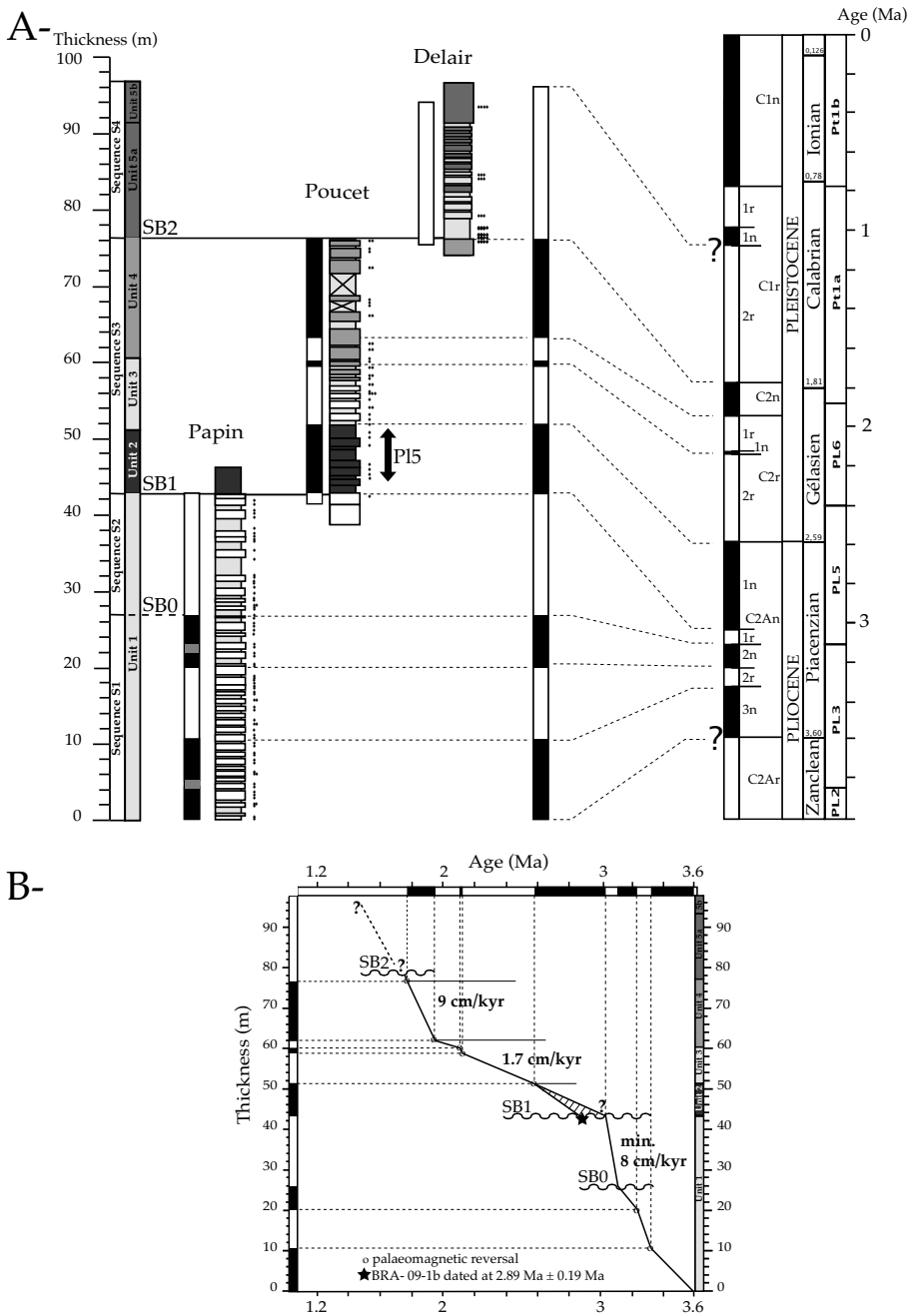

Fig. 6. (**a**) Correlation of the polarity sequence of the studied sections and the derived composite magnetostratigraphy to the GPTS. (**b**) Estimation of mean accumulation rates of carbonate platforms in Grande-Terre. The legend for stratigraphic columns is as for Figure 5; diamonds indicate sample locations.

the hiatus associated with the hardground is *c*. 400 kyr. Correlatively, it is demonstrated that deposition of Unit 4 started *c*. 200 kyr earlier in the western part (Poucet section) than in the eastern part (Anse à l'Eau section) of the forearc (Fig. 7) in agreement with the overall eastward prograding geometry of Unit 4. Moreover, it appears that the sediment accumulation rates varied across the forearc.

Sequence S3 also crops out in Marie-Galante, Petite-Terre and La Désirade. In La Désirade, a Pleistocene age has been proposed on the basis of the occurrence of the coral *Diploria labyrinthiformis* (Lardeaux *et al.*, 2013), in agreement with our results from Grande-Terre. We further propose that the deposition of sequence S3 occurred between *c*. 2.9 and 1.77 Ma in this part of the forearc.

Sequence S4

The duration of the hiatus associated with unconformity SB2 cannot be estimated owing to poor absolute age constraints in Sequence S4 (Unit 5). However, samples BC-1 and BC-2 from the upper part of this sequence yielded calcareous nannofossil assemblages of Calabrian age (Münch *et al.* 2013) and $^{40}Ar/^{39}Ar$ ages at 1.33 ± 0.23 and 1.15 ± 0.12 Ma (Fig. 3d and e), respectively. Because the whole Delair section (Units 5a and b) is reversely magnetized, this suggests that the deposition of S4 occurred within Subchron C1r.2r during the Calabrian before the beginning of Subchron C1r.1n (Jaramillo) at 1.07 Ma. This is in accordance with previous biostratigraphic analyses by Andreieff *et al.* (1989). The sequence S4, corresponding to the 'upper plateaux' of Feuillet *et al.* (2002, 2004), ended before 1.07 Ma and not during the 330 ka highstand as proposed by those researchers. The occurrence of sequence S4 on all islands suggests that the definite emergence of the Guadeloupe archipelago occurred during Subchron C1r.2r. Following Cornée *et al.* (2012), who suggested that SB2 could be correlated with the glacio-eustatic Cala1 lowstand (Haq *et al.* 1988), the definite emergence may then have occurred during the Cala2 lowstand at

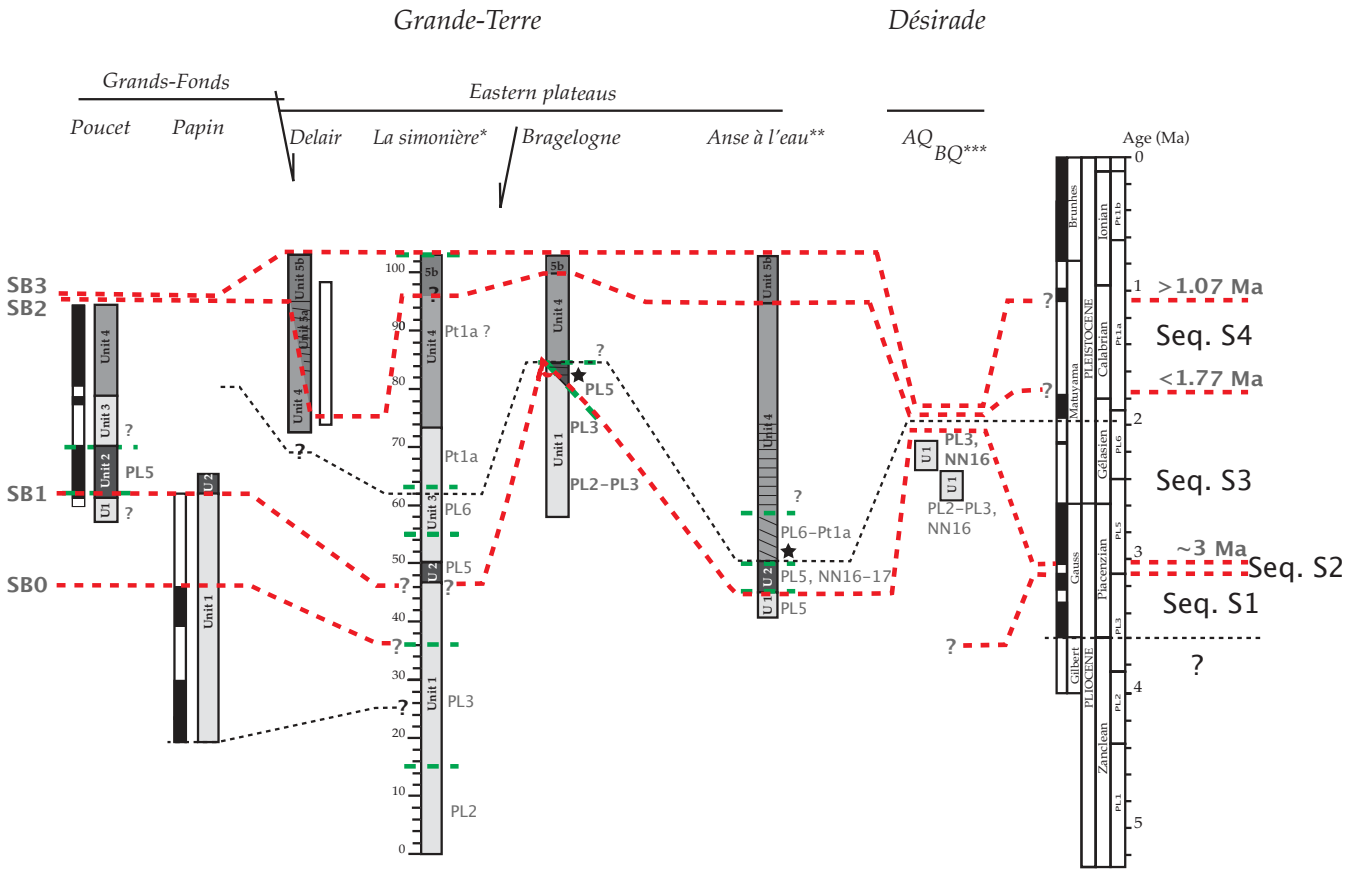

Fig. 7. Stratigraphy, sequence stratigraphy and biostratigraphy of the Pliocene to Pleistocene carbonate platforms in Grande-Terre, and correlation of the polarity sequence of the studied sections to the GPTS. Black star, location of dated crystal tuffs (this study). Foraminifera and nannofossil zones are shown in bold type: this study; *biostratigraphic data from La Simonière drill after Andreieff *et al.* (1989); **biostratigraphic data from Cornée *et al.* (2012); ***biostratigraphic data from Lardeaux *et al.* (2013).

1.54 Ma (recalibrated age of Lugowski *et al.* 2011). In addition, the occurrence of deep-water pelagic Calabrian sediments in the Marie-Galante basin indicates that a deep basin already existed there at this time and that it was not only recently created.

Tectonostratigraphy of the Guadeloupe forearc and relationships with volcanic activity

Our integrated stratigraphy of the carbonate platforms of the Guadeloupe archipelago helps to constrain the tectonics of the Lesser Antilles forearc. At least three main extensional episodes occurred between the late Tortonian and the middle Pleistocene (Calabrian) and are interrelated with the various volcanic building phases of Basse-Terre.

Late Miocene–late Pliocene

A first, still weakly constrained, extensional episode occurred during the late Tortonian–Messinian interval (i.e. between 8.6 and 5.3 Ma). This episode is mainly observable in La Désirade, where N130°E-striking normal faults were active before the deposition of sequence S1 (Fig. 8; Lardeaux *et al.* 2013). These faults were inherited from a dextral strike-slip shear zone in the Cretaceous metavolcanic basement (Lardeaux *et al.* 2013). The occurrence of deformed and eroded late Tortonian marine sediments in Marie-Galante (sample AP-1) indicates that this first extensional episode was coeval with uplift and emergence of most parts of the forearc. This is also supported by the presence of a subaerial erosional surface at the top of the basement in La Désirade (Lardeaux *et al.* 2013). Deposition of sequences S1 and S2 occurred during the early–late Pliocene, when the forearc underwent subsidence with a mean vertical accumulation rate estimated at 8 cm ka^{-1} in Grande-Terre (Fig. 6b). The thickness of these sequences changes from one island to another: >50 m in Grande-Terre, 120 m in La Désirade and 190 m in Marie-Galante. Considering that sequences S1 and S2 have the same duration in the whole archipelago, subsidence rates were presumably not uniform at the scale of the forearc.

Latest Pliocene (late Piacenzian)–early Pleistocene (Gelasian)

A second major extensional episode occurred soon before and/or during the deposition of the basal part of Sequence S3 (Unit 2); that is, at *c.* 3 Ma. The N130°E-striking normal faults were reactivated at least in La Désirade and in the eastern part of Grande-Terre. This tectonic episode was coeval with the uplift of the forearc that led to the emergence of the eastern part of Grande-Terre and of La Désirade as exemplified by the erosion of deposits from previous sequences (sequences S1 or S2) in the footwall of N130°E normal faults (Fig. 8b). The uplift was more pronounced in the eastern part of the forearc, for example in La Désirade, where deposits from sequence S2 were completely eroded whereas they were preserved in Grande-Terre (Fig. 8b). This extensional tectonic activity ended during the late Gelasian as exemplified by the unconformable

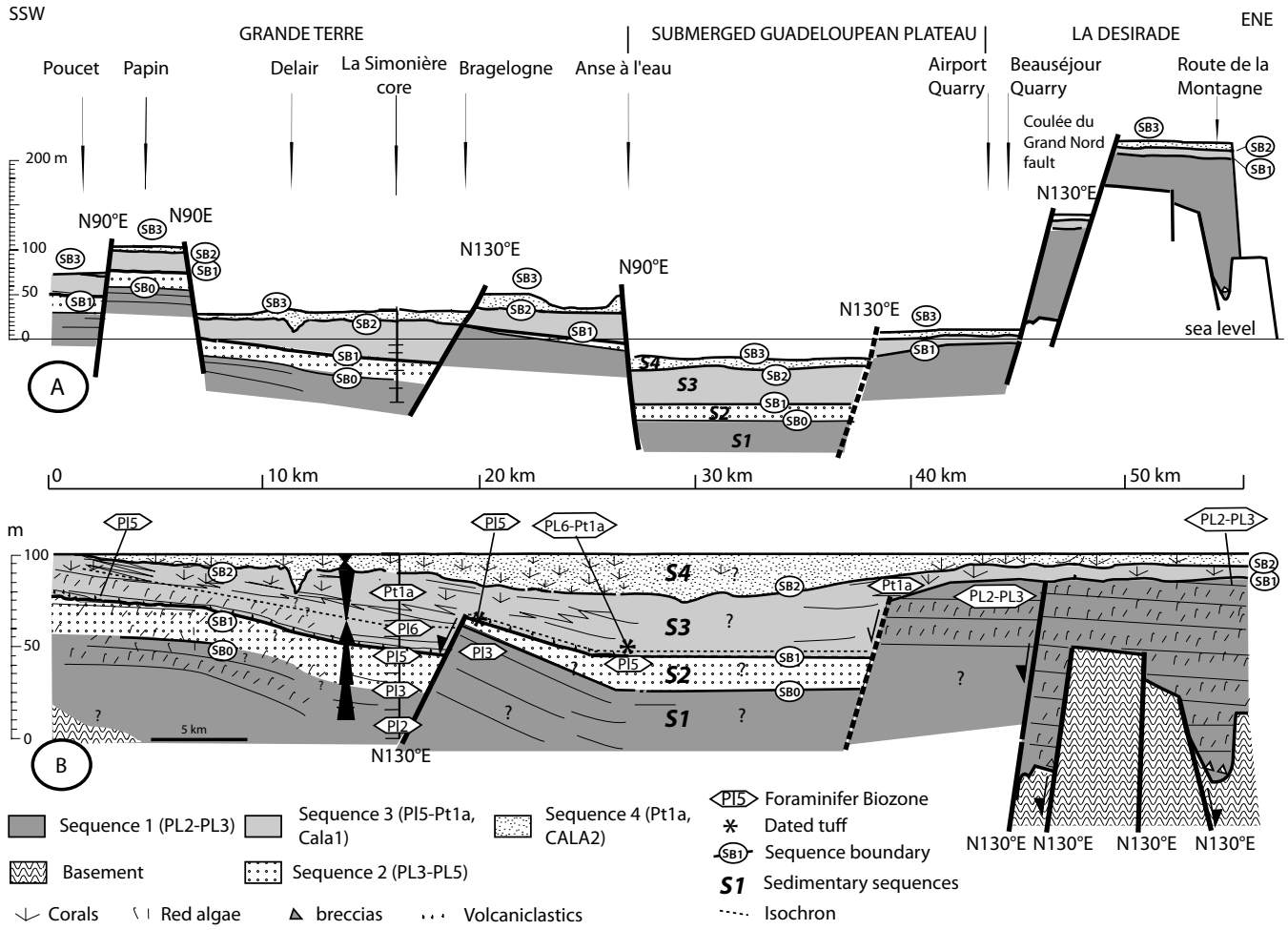

Fig. 8. Simplified general cross-sections of carbonate platforms throughout the forearc, from Grande-Terre to La Désirade: (**a**) at the present day; (**b**) at the time of Sequence S4 highstand, prior to the last, still active, extensional tectonic episode.

development of prograding reefs (Unit 4, sequence S3) above the faulted and eroded earlier deposits (Fig. 8b).

This tectonic episode was roughly synchronous with the aerial volcanic activity in the Basse-Terre arc in Basse-Terre. Indeed, the initial subaerial volcanism in Basse-Terre was dated from 2.79 ± 0.08 to 2.68 ± 0.08 Ma (described as Basal Complex activity by Samper *et al.* 2007). The volcanoclastic deposits of Unit 2 of Grande-Terre (sample BRA-09-1b: 2.89 ± 0.19 Ma) are then coeval with the Basal Complex. The continental depositional environment of Unit 2 in the westernmost part of Grande-Terre definitely confirms the emergence of the volcanic arc at this time.

Middle Pleistocene (Calabrian)–Present

A third extensional tectonic episode occurred since the Middle Pleistocene. Its dating is crucial because it corresponds to the active present-day extensional regime, and because it coincides both with the formation of the present-day Marie-Galante basin and with the final emergence of the carbonate platforms. This tectonic episode is characterized by the formation of east–west-striking normal faults but also by the reactivation of N130°E-striking faults (Fig. 8a). This tectonic episode started much earlier than *c*. 0.5 Ma as proposed by Feuillet *et al.* (2002, 2004) but before *c*. 1.5 Ma. Moreover, those researchers assumed an age of 330 ka for the final emergence to calculate uplift rates and fault slip rates. However, we have shown that this emergence occurred much earlier, before 1.07 Ma, and probably at *c*. 1.5 Ma. Thus, fault slip rates and uplift rates have to be more than three times lower than previously proposed (Feuillet *et al.* 2004).

This third tectonic episode is contemporaneous with some volcanic activity in Basse-Terre that was dated to 1.81 ± 0.06 to 1.15 ± 0.04 Ma (the Septentrional Chain of Samper *et al.* 2007). Our results show that this volcanic episode was also recorded within carbonate platform deposits and we dated it between 1.96 ± 0.17 and 1.15 ± 0.15 Ma. The NNW–SSE-trending linear shape of the Septentrional Chain could then be related to the Middle Pleistocene tectonic episode as already proposed for the localization of the most recent volcanic complex (Feuillet *et al.* 2002).

Extensional tectonics thus occurred since at least the late Miocene in this part of the Lesser Antilles forearc. It appears that the development of the volcanic arc was closely interrelated to extensional tectonics since the Pliocene. Between tectonic episodes, the forearc was subjected to subsidence that led to the development of isolated carbonate platforms on topographic highs and to a pelagic sedimentation in the Marie-Galante graben. This general subsidence of the forearc was interrupted by repeated uplift phases. However, our results concern only the carbonate platforms that developed on late Miocene structural highs, where subsidence was lower than in the neighbouring basinal areas. Subsidence requires forearc thinning and it has been proposed that it was related to tectonic erosion of the

base of the overriding plate (Clift & Vannucchi 2004). It has also been proposed that the response of forearcs to aseismic ridge subduction may be subsidence interrupted by rapid uplift episodes (Vannucchi *et al.* 2013). The study of such a subduction dynamics process is beyond the scope of this paper, but our results confirm that subsidence and extensional deformation in this part of the forearc were long-term processes. The two first tectonic episodes cannot be interpreted in terms of arc-parallel extension because of the geometry of N130°E normal faults that reactivated older basement faults (Lardeaux *et al.* 2013). Instead, they were probably related to subduction erosion linked to the subduction of the Tiburon aseismic ridge (Fig. 1). The final tectonic episode was characterized by east–west normal faults indicating an arc-parallel extension but also by the reactivation of N130°E normal faults. It was also associated with rapid uplift, suggesting that subduction erosion processes may still contribute to extensional deformation of the forearc. Thus, interpretations of the Pliocene to present-day extensional regime in the Guadeloupe archipelago should be refined.

Conclusion

The tectonic evolution of the Guadeloupe forearc is characterized by an overall subsidence and repeated episodes of extension since the late Miocene. Three main extensional episodes occurred and were associated with local uplift that created forearc highs on which early Pliocene to middle Pleistocene carbonate platforms developed. At the scale of the study region the deformations related to the two first episodes are more important in the eastern part of the forearc towards the trench, whereas the effects of the third episode are mainly identified in the western part towards the volcanic arc. The carbonate platforms were subsequently uplifted and partly emerged. Integrated stratigraphy of carbonate platforms constrains the timing of the deformation of the forearc during the last *c*. 8 myr.

The timing of the first episode remains loosely constrained as late Tortonian–Messinian, but it is important because it was responsible for the formation of the initial palaeotopography on which the carbonate platforms began to develop. N130°E-striking normal faults were the main deformation features linked to this episode. Following this episode, a period of subsidence of the whole forearc occurred with highest subsidence rates toward the trench.

The second tectonic episode occurred at around 3 Ma. It corresponded to the development of the subaerial volcanic activity in the arc. It was also dominated by N130°E-striking normal faulting and led to the emergence of most parts of the carbonate platforms and mainly of La Désirade. Then, the subsidence resumed mainly in the western part of the forearc, near the active volcanic chain, but at a slower rate.

The last episode of deformation led to the demise of the carbonate platforms before 1.07 Ma, and perhaps at *c*. 1.5 Ma (Cornée *et al.* 2012), related to the onset of arc-parallel extension. It corresponds to the uplift of all islands of the archipelago and the subsidence of the Marie-Galante Basin over an inherited trough. During this period the forearc did not undergo a general westward tilting but was deformed in a more complex way, with the growth of east–west-oriented normal faults and the reactivation of inherited N130°E structures. This structural inheritance is obviously linked to the nature of the substratum of the forearc as N130°E-striking faults correspond to a Cretaceous strike-slip shear zone in La Désirade (Corsini *et al.* 2011; Lardeaux *et al.* 2013).

The proposed tectonostratigraphic model of the Guadeloupe forearc corresponds to mature stages of forearc-basin development (Dickinson 1995; Dorobek 2008). The regional subsidence of this part of the forearc that was associated with extensional tectonics and rapid uplift events may be related to tectonic erosion at the subduction interface.

This work was funded the French National Program DyETI, the French INSU-Campagnes à la Mer project 'KaShallow', the French INSU-SYSTER project 'Vertical motion in forearcs: frontal subduction vs oblique subduction', the European Interreg IIIB 'Caribbean Space' and FEDER (op. 30-700) projects as well as by the Region Guadeloupe. The authors thank two anonymous reviewers and Subject Editor J. Hendry.

References

Andreieff, P., Bouysse, P. & Westercamp, D. 1983. Révision géologique de l'île de Marie-Galante (Petite Antilles). *Bulletin de la Société Géologique de France*, **XXV**, 805–810.

Andreieff, P., Bouysse, P. & Westercamp, D. 1989. *Géologie de l'arc insulaire des Petites Antilles et évolution géodynamique de l'Est-Caraïbe*. Documents du Bureau de Recherches Géologiques et Minières, **171**.

Berggren, W.A., Kent, D.V., Swisher, C.C., III & Aubry, M.P. 1995. A revised Cenozoic geochronology and chronostratigraphy. *In*: Berggren, W.A., Kent, D.V., Aubry, M.P. & Hardenbol, J. (eds) *Geochronology, Time Scales and Global Stratigraphic Correlation*. Society of Economic Paleontologists and Mineralogists, Special Publications, **54**, 129–212.

Bouysse, P. & Garrabé, F. 1984. Evolution tectonique néogène des îles calcaires de l'archipel de la Guadeloupe. *Comptes Rendus de l'Académie des Sciences, Série IIA*, **298**, 763–766.

Bouysse, P. & Westercamp, D. 1990. Subduction of Atlantic aseismic ridges and Late Cenozoic evolution of the Lesser Antilles island arc. *Tectonophysics*, **175**, 349–380.

Bouysse, P., Schmidt-Effing, R. & Westercamp, D. 1983. La Desirade Island (Lesser Antilles) revisited: Lower Cretaceous radiolarian cherts and arguments against an ophiolitic origin for the basal complex. *Geology*, **11**, 244–247.

Bouysse, P., Westercamp, D. & Andreieff, P. 1990. The Lesser Antilles island arc. *In*: Mascle, A., Moore, J.C., *et al.* (eds) Proceedings of the Ocean Drilling Program, Scientific Results, **110**, 29–44.

Bouysse, P., Garrabé, F. & Mauboussin, T. 1993. *Carte géologique de la France (1/50000), Feuille Marie-Galante et îlets de la Petite-Terre (Guadeloupe)*. Service Géologique National. Bureau de Recherches Géologiques et Minières, Orléans.

Cas, R.A.F. & Wright, J.V. 1988. *Volcanic Successions, Modern and Ancient*. Unwin Hyman, London.

Clift, P. & Vannucchi, P. 2004. Controls on tectonic accretion versus erosion in subduction zones: Implications for the origin and recycling of the continental crust. *Reviews of Geophysics*, **42**, RG 2001, http://dx.doi.org/10.1029/2003RG000127.

Cordey, F. & Cornée, J.-J. 2009. Late Jurassic radiolarians from La Desirade basement complex (Guadeloupe, Lesser Antilles Arc) and tectonic implications. *Bulletin de la Societe Géologique de France*, **180**, 399–409.

Cornée, J.-J., Münch, Ph., *et al.* 2006. Timing of Late Pliocene to Middle Pleistocene tectonic events in Rhodes (Greece) inferred from magnetobiostratigraphy and $^{40}Ar/^{39}Ar$ dating of a volcaniclastic layer. *Earth and Planetary Science Letters*, **250**, 185–195.

Cornée, J.-J., Léticée, J.-L., *et al.* 2012. Sedimentology, palaeoenvironments and biostratigraphy of the Pliocene–Pleistocene carbonate platform of Grande-Terre (Guadeloupe, Lesser Antilles forearc). *Sedimentology*, **59**, 1426–1451.

Corsini, M., Lardeaux, J.M., Vérati, C., Voitus, E. & Balagne, M. 2011. Discovery of Lower Cretaceous synmetamorphic thrust tectonics in French Lesser Antilles (La Désirade Island, Guadeloupe): Implications for Caribbean geodynamics. *Tectonics*, **30**, TC4005, http://dx.doi.org/10.1029/2011TC002875.

Cunningham, K.J., Farr, M.R. & Rakic-ElBied, K. 1994. Magnetostratigraphic dating of an upper Miocene shallow-marine and continental sedimentary succession in northeastern Morocco. *Earth and Planetary Science Letters*, **127**, 77–93.

De Mets, C., Jansma, P.E., *et al.* 2000. GPS geodetic constraints on Caribbean–North America plate motion. *Geophysical Research Letters*, **27**, 437–440.

Dickinson, W.R. 1995. Forearc basins. *In*: Busby, C.J. & Ingersoll, R.V. (eds) *Tectonics of Sedimentary Basins*. Blackwell Science, Cambridge, MA, 221–261.

Dorobek, S.L. 2008. Carbonate-platform facies in volcanic-arc settings: Characteristics and controls on deposition and stratigraphic development. *In*: Draut, A.E., Clift, P.D. & Scholl, D.W. (eds) *Formation and Applications of the Sedimentary Record in Arc Collision Zones*. Geological Society of America, Special Papers, **436**, 55–90, http://dx.doi.org/10.1130/2008.2436(04)

Feuillet, N., Manighetti, I. & Tapponnier, P. 2002. Arc parallel extension and localization of volcanic complexes in Guadeloupe, Lesser Antilles. *Journal of Geophysical Research*, **107**, 2331, http://dx.doi.org/10.1029/2001JB000308.

Feuillet, N., Tapponnier, P., Manighetti, I., Villemant, B. & King, G.C.P. 2004. Differential uplift and tilt of Pleistocene reef platforms and Quaternary slip

rate on the Morne-Piton normal fault (Guadeloupe, French West Indies). *Journal of Geophysical Research*, **109**, BO2404.

Fisher, R. 1953. Dispersion on a sphere. *Proceedings of the Royal Society of London, Series A*, **217**, 295–305.

Garrabé, F. & Andreieff, P. 1985. Sédimentation et tectonique Plio-Quaternaires comparées de Marie-Galante et de Grande-Terre (Guadeloupe). *In*: Mascle, A. (ed.) *Géodynamique des Caraïbes, Symposium*. Technip, Paris, 155–160.

Garrabé, F. & Andreieff, P. 1988. *Carte géologique de la France (1/50000), Feuille Grande-Terre (Guadeloupe)*. Service Géologique National, Bureau de Recherches Géologiques et Minières, Orléans.

Haq, B.U., Hardenbol, J. & Vail, P.R. 1988. Mesozoic and Cenozoic chronostratigraphy and cycles of sea level change. *In*: Wilgus, C.K., Hastings, B.S., Kendall, C.G.St.C., Posamentier, H., Ž. Ross, C.A. & van Wagoner, J. (eds) *Sea Level Changes—An Integrated Approach*. Society of Economic Paleontologists and Mineralogists, Special Publications, **42**, 71–108.

Kennett, J.P. & Srinivasan, M.S. 1983. *Neogene Planktonic Foraminifers: A Phylogenic Atlas*. Hutchinson Ross, New York.

Kirschvink, J.L. 1980. The least-squares line and plane and the analysis of palaeomagnetic data. *Geophysical Journal of the Royal Astronomical Society*, **62**, 699–718.

Koppers, A.A.P. 2002. ArArCALC-software for $^{40}Ar/^{39}Ar$ age calculations. *Computers and Geosciences*, **28**, 605–619.

Lardeaux, J.-M., Münch, Ph., *et al.* 2013. La Désirade Island (Guadeloupe, French West Indies): A key target for deciphering the role of reactivated tectonic structures in Lesser Antilles arc building. *Bulletin de la Société Géologique de France*, **184**, 21–34.

Léticée, J.-L., Randrianasolo, A., *et al.* 2005. Mise en évidence d'une discontinuité émersive majeure au sein de la plate-forme récifale Plio-Pléistocène l'avant-arc des Petites Antilles. *Comptes Rendus de l'Académie des Sciences, Série IIA*, **337**, 617–624.

Lourens, L., Hilgen, F., Shackleton, N.J., Laskar, J. & Wilson, D. 2004. The Neogene Period. *In*: Gradstein, F.M., Ogg, J.G. & Smith, A.G. (eds) *A Geologic Time Scale*. Cambridge University Press, Cambridge, 409–440.

Lugowski, A., Ogg, J., Gradstein, F.M. & Ault, A. 2011. Time Scale Creator 4.2.5 software. http://www.tscreator.org.

Mann, P., Taylor, F.W., Edwards, R.L. & Ku, T.L. 1995. Actively evolving microplate formation by oblique collision and sideways motion along strike-slip fault: An example from the Northeastern Caribbean plate margin. *Tectonophysics*, **246**, 1–69.

Martini, E. 1971. Standard Tertiary and Quaternary calcareous nannoplankton zonation. *In*: Farinacci, A. (ed.) *Proceedings of the Second International Conference on Planktonic Microfossils Roma, Rome*. Edizioni Tecnoscienza, **2**, 739–785.

Mattinson, J.M., Fink, L.K., Jr. & Hopson, C.A. 1980. Geochronologic and isotopic study of the La Desirade Island basement complex. Jurassic oceanic crust in the Lesser Antilles. *Contributions to Mineralogy and Petrology*, **71**, 237–245.

Mattinson, J.M., Pessagno, E.A., Jr., Montgomery, H. & Hopson, C.A. 2008. Late Jurassic age of oceanic basement at La Désirade Island, Lesser Antilles arc. *In*: Wright, J. & Shervais, J. (eds) *Ophiolites, Arcs, and Batholiths: a Tribute to Cliff Hopson*. Geological Society of America, Special Papers, **438**, 175–190.

McFadden, P.L. & McElhinney, M.W. 1988. The combined analysis of remagnetization circles and direct observations in palaeomagnetism. *Earth and Planetary Science Letters*, **87**, 161–172.

Menabreaz, A., Thouveny, N., Camoin, G. & Lund, S.P. 2010. Paleomagnetic record of the late Pleistocene reef sequence of Tahiti (French Polynesia): A contribution to the chronology of the deposits. *Earth and Planetary Science Letters*, **294**, 58–68.

Münch, Ph., Lebrun, J.-F., Cornée, J.-J., Thinon, I., Guennoc, P., Marcaillou, B. & Randrianasolo, A. 2013. Pliocene to Pleistocene carbonate systems of the Guadeloupe archipelago, French Lesser Antilles: a land and sea study. *Bulletin de la Société Géologique de France*, **184**, 99–110.

Okada, H. & Bukry, D. 1980. Supplementary modification and introduction of code numbers to the Low Latitude Coccolith Biostratigraphy Zonation (Bukry, 1973, 1975). *Marine Micropaleontology*, **51**, 321–325.

Oudet, J., Münch, Ph., *et al.* 2010. Integrated chronostratigraphy of an intra-arc basin: $^{40}Ar/^{39}Ar$ datings, micropalaeontology and magnetostratigraphy of the early Miocene Castelsardo basin (northern Sardinia, Italy). *Palaeogeography, Palaeoclimatology, Palaeoecology*, **295**, 293–306.

Perch-Nielsen, K. 1985. Cenozoic calcareous nannofossils. *In*: Bolli, H., Saunders, J. & Perch-Nielsen, K. (eds) *Plankton Stratigraphy*. Cambridge University Press, Cambridge, 428–514.

Pindell, J.L. & Kennan, L. 2009. Tectonic evolution of the Gulf of Mexico, Caribbean and northern South America in the mantle reference frame: an update. *In*: James, K.H., Lorente, M.A. & Pindell, J.L. (eds) *The Origin and Evolution of the Caribbean Plate*. Geological Society, London, Special Publications, **328**, 1–55.

Prevot, M. 1981. Some aspects of magnetic viscosity in subaerial and submarine volcanic rocks. *Geophysical Journal of the Royal Astronomical Society*, **66**, 169–192.

Raffi, I., Backman, J., Fornaciari, E., Pälike, H., Rio, D., Lourens, L. & Hilgen, F. 2006. A review of calcareous nannofossil astrobiochronology encompassing the past 25 million years. *Quaternary Science Review*, **25**, 3113–3137.

Renne, P.R., Mundil, R., Balco, G., Min, K. & Ludwig, K.R. 2010. Joint determination of ^{40}K decay constants and $^{40}Ar^*/^{40}K$ for the Fish Canyon sanidine standard, and improved accuracy for $^{40}Ar/^{39}Ar$ geochronology. *Geochimica et Cosmochimica Acta*, **74**, 5349–5367, http://dx.doi.org/10.1016/j.gca.2010.06.017.

Samper, A., Quidelleur, X., Lahitte, P. & Mollex, D. 2007. Timing of effusive volcanism and collapse events within an oceanic arc island: Basse-Terre, Guadeloupe archipelago (Lesser Antilles Arc). *Earth and Planetary Science Letters*, **258**, 175–191.

Vannucchi, P., Sak, P.B., Morgan, J.P., Ohkushi, K. & Ujiie, K. & IODP Expedition 334 Shipboard Scientists. 2013. Rapid pulses of uplift, subsidence, and subduction erosion offshore Central America: Implications for building the rock record of convergent margins. *Geology*, **41**, 995–998.

Wade, B.S., Pearson, P.N., Berggren, W.A. & Pälike, H. 2011. Review and revision of Cenozoic tropical planktonic foraminiferal biostratigraphy and calibration to the geomagnetic polarity and astronomical time scale. *Earth-Science Reviews*, **104**, 111–142.

Westercamp, D. 1980. *La Désirade, carte géologique à 1:25000 et notice explicative*. Service Géologique National, Bureau de Recherches Géologiques et Minières, Orléans, France.

Young, J., Geisen, M., Cors, L., Klijne, A., Sprengel, C., Probert, I. & Osternngaard, J. 2003. A guide to extant coccolithophores taxonomy. *Journal of Nannoplankton Research, Special Issue*, **1**, 125.

Zijderveld, J.D.A. 1967. A.C. demagnetization of rocks: analysis of results. *In*: *Methods in Paleomagnetism*. Elsevier, Amsterdam, 254–286.